Research Repository UCD

Title	A Fully Integrated GaN Dual-Channel Power Amplifier With Crosstalk Suppression for 5G Massive MIMO Transmitters
Authors(s)	Nikandish, Gholamreza, Staszewski, Robert Bogdan, Zhu, Anding
Publication date	2021-01
Publication information	Nikandish, Gholamreza, Robert Bogdan Staszewski, and Anding Zhu. "A Fully Integrated GaN Dual-Channel Power Amplifier With Crosstalk Suppression for 5G Massive MIMO Transmitters." IEEE, January 2021. https://doi.org/10.1109/tcsii.2020.3008365.
Publisher	IEEE
Item record/more information	http://hdl.handle.net/10197/12022
Publisher's statement	© 2020 IEEE. Personal use of this material is permitted. Permission from IEEE must be obtained for all other uses, in any current or future media, including reprinting/republishing this material for advertising or promotional purposes, creating new collective works, for resale or redistribution to servers or lists, or reuse of any copyrighted component of this work in other works.
Publisher's version (DOI)	10.1109/tcsii.2020.3008365

Downloaded 2026-05-02 01:15:32

The UCD community has made this article openly available. Please share how this access benefits you. Your story matters! (@ucd_oa)

© Some rights reserved. For more information

A Fully Integrated GaN Dual-Channel Power Amplifier With Crosstalk Suppression for 5G Massive MIMO Transmitters

G. Reza Nikandish, *Senior Member, IEEE,* Robert Bogdan Staszewski, *Fellow, IEEE,* and Anding Zhu, *Senior Member, IEEE*

***Abstract*—We present a broadband dual-channel power amplifier (PA) with crosstalk suppression for multi-input multi-output (MIMO) communications. Operation of MIMO system with crosstalk is theoretically evaluated for two popular coding schemes including the space-time coding and linear precoding. Design challenges of a multi-channel PA on a single chip are investigated and circuit techniques, including second-harmonic trapping integrated into the output matching network and the use of back-via lines to isolate the channels, are proposed to mitigate the inter-channel crosstalk. A fully integrated dual-channel PA prototype, implemented using a 250-nm GaN-on-SiC process, provides 34.9–36.3 dBm output power, 44–49% power-added efficiency (PAE), 11.3–12.3 dB power gain, 31.0–34.2 dB second-harmonic rejection, and −28.1 dB to −25.7 dB inter-channel crosstalk across 4.5–6.5 GHz. For a 100-MHz 256-QAM signal with 7.2 dB peak-to-average power ratio (PAPR), the PA achieves 29.9 dBm average output power, 30% average PAE, −38.2/−39.1 dBc adjacent channel leakage ratio (ACLR), and −28.2 dB (3.9%) rms error vector magnitude (EVM), without using digital predistortion (DPD). Effect of crosstalk on linearity of the dual-channel PA is also measured and it is shown that for a 256-QAM signal EVM can increase by 3–8 dB, depending on relative power levels of the two channels.**

***Index Terms*—5G, broadband amplifier, crosstalk, GaN, multi-input multi-output (MIMO), power amplifier (PA), transmitter.**

I. Introduction

THE continuous growth in the demand for wireless connectivity has led to the emergence of the Fifth Generation (5G) wireless networks. A multi-input multi-output (MIMO) system is one of the key enabling technologies for 5G. MIMO can be used either in spatial diversity or spatial multiplexing mode. The spatial diversity can extend the coverage range by transmitting the same information over all transmitter (TX) antennas, while in the spatial multiplexing independent signals are simultaneously transmitted over the same frequency to increase spectral efficiency. Massive MIMO with a large number of TX and receiver (RX) antennas is used in 5G [1].

It is desired to integrate multiple TX and/or RX front-end channels on a single chip. Such integration provides numerous advantages including lower variations in performance of different channels, ease of system calibration, lowered fabrication costs, and compact hardware implementation [2]. Several integrated MIMO front-ends including transceivers and multi-channel power amplifiers (PAs) are reported in the literature [3], [4], [5]. Most of these circuits are implemented using mainstream silicon technologies to achieve low cost and high level of integration. However, these process technologies suffer from low output power levels, low efficiency, and high crosstalk between channels as a result of lossy substrate. GaN monolithic microwave integrated circuit (MMIC) technology is an attractive solution for 5G systems, especially for base-station PAs [6], [7], [8], where it can provide high output power levels in a compact chip area. Furthermore, the lower losses of its SiC substrate help to reduce crosstalk in a multi-channel PA, which has been shown to have the most detrimental effect on the performance of MIMO systems [5]. Although some crosstalk cancellation techniques have been developed for MIMO transmitters using digital a predistortion (DPD), e.g., [9], it is still essential to achieve high linearity and low crosstalk at the *raw* circuit-level implementation.

In this paper, we present design and implementation of a dual-channel monolithic GaN PA for 5G MIMO transmitters. The new contributions can be summarized as follows.

1) A crosstalk theory based on signal-to-noise ratio (SNR) is developed to benchmark performance of a 2×2 MIMO communication system for two popular coding schemes, Alamouti space-time coding [10] and linear precoding [11].
2) A crosstalk reduction technique is proposed for multi-channel PAs by embedding a broadband second-harmonic filter into the PA output matching network.
3) A line of back-vias available in monolithic GaN processes is used to mitigate the parasitic transformer coupling between the channels.
4) The crosstalk and its effects on the dual-channel PA performance are characterized using both continuous-wave and modulated-signal measurements, first time ever in the GaN process.

The paper is organized as follows. In Section II, design considerations for a single-chip multi-channel PA are presented. Design of the PA circuitry with harmonic filter is described in Section III. Finally, in Section IV, we provide single- and dual-channel measurement results.

II. Multi-Channel PA Design for MIMO TX

A. Operation of MIMO System with Crosstalk

The block diagram of a 2×2 MIMO communication system is shown in Fig. 1. It is used as a demonstrator of the crosstalk

This research has received funding from the European Union's Horizon 2020 Research and Innovation Program under the Marie Sklodowska-Curie grant agreement number 713567, and Science Foundation Ireland (SFI) under grant numbers 13/RC/2077 and 16/IA/4449.

The authors are with the School of Electrical and Electronic Engineering, University College Dublin, Ireland (e-mail: nikandish@ucd.ie, robert.staszewski@ucd.ie, anding.zhu@ucd.ie).

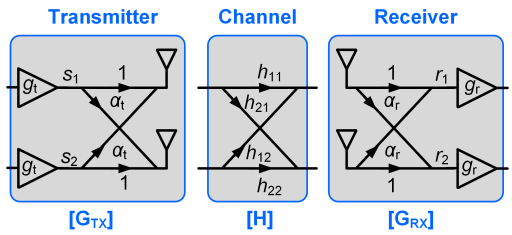

Fig. 1. Block diagram of a 2×2 MIMO communication system.

issue in a practical multi-channel MIMO system. We derive the output SNR in terms of input SNR and the system parameters. The TX, RX, and the channel can be modeled by the matrices $[G_{TX}]$, $[G_{RX}]$, and $[H]$, respectively. Assuming symmetric TX channels, the TX system can be modeled by a direct gain of g_t and a coupled gain of α_t. Similarly, the RX system can be modeled by parameters g_r and α_r. The system can be modeled by an equivalent channel matrix of

$$[H_e] = \begin{bmatrix} 1 & \alpha_t \\ \alpha_t & 1 \end{bmatrix} \begin{bmatrix} h_{11} & h_{12} \\ h_{21} & h_{22} \end{bmatrix} \begin{bmatrix} 1 & \alpha_r \\ \alpha_r & 1 \end{bmatrix}. \quad (1)$$

The physical channel matrix $[H]$ is practically determined for specific propagation conditions. Assuming a lossless symmetric channel, we use the following model

$$[H] = \begin{bmatrix} \sqrt{1-k^2} & ke^{-j\theta_h} \\ ke^{-j\theta_h} & \sqrt{1-k^2} \end{bmatrix}, \quad (2)$$

where two parameters $0 \le k \le 1$ and $0 \le \theta_h < 2\pi$ can be used to investigate the effect of channel behavior on the MIMO system with crosstalk. The parameter k indicates the strength of correlation between the two channels. A case of $k = 0$ refers to two uncorrelated single-input single-output (SISO) channels. Moreover, the parameter θ_h captures a relative phase shift between the main and cross paths. To proceed, we consider two popular coding schemes, Alamouti space-time coding [10] and linear precoding [11], and derive the SNR loss due to crosstalk.

1) Alamouti Space-Time Coding: Assuming the Alamouti space-time coding scheme with a maximum likelihood detector, the received signal matrix $[R]$ is given by

$$[R] = [H_e][S] + [N], \quad (3)$$

where $[S]$ denotes the transmitted signal matrix and $[N]$ is the additive channel noise matrix. The TX crosstalk has the most detrimental effect on the quality of detected signal [5]. By neglecting the RX crosstalk ($\alpha_r = 0$), and considering the TX crosstalk as $\alpha_t = |\alpha_t|e^{-j\theta_t}$, it can be shown that the SNR loss due to the crosstalk is derived as follows

$$\Delta\text{SNR} = -10\log_{10}\left(1 + |\alpha_t|^2 + 4|\alpha_t|k\sqrt{1-k^2}\cos\theta_h\cos\theta_t\right). \quad (4)$$

In the case of $k = 0$, the crosstalk should be lower than -6.6 dB to limit the SNR loss to 0.2 dB. The maximum SNR loss condition can be derived from $\partial(\Delta\text{SNR})/\partial k = 0$, which leads to $k = 1/\sqrt{2}$. Using this value and $\cos\theta_h = \cos\theta_t = \pm 1$ in (2), the maximum SNR loss is given by

$$\Delta\text{SNR}_{max} = -20\log_{10}\left(1 + |\alpha_t|\right). \quad (5)$$

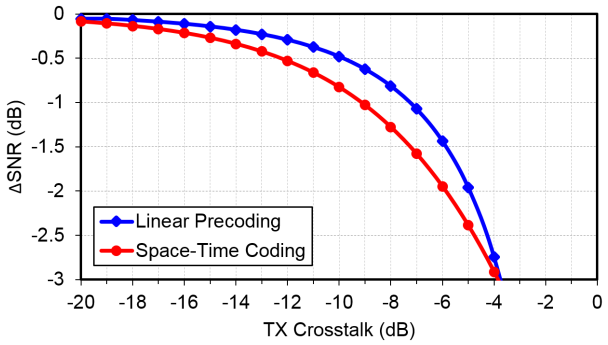

Fig. 2. SNR loss of MIMO system versus TX crosstalk (for the worst case of $k = 1/\sqrt{2}$) for two popular coding schemes: Alamouti space-time coding [10] and linear precoding with matched filter [11].

This is shown in Fig. 2, which indicates that < -16.3 dB crosstalk is required to maintain the SNR loss < 0.2 dB.

2) Linear Precoding: In the case of linear precoding with matched filter, the received signal is given by

$$[R] = [H]^H[H_e][S] + [N], \quad (6)$$

where precoder matrix $[H]^H$ is the Hermitian (conjugate transpose) of the physical channel matrix. It can be shown that the SNR loss due to the TX crosstalk is derived as

$$\Delta\text{SNR} = -10\log_{10}\left(\frac{|\alpha_t + \beta|^2 + 1}{|1 + \alpha_t\beta|^2(1+\beta^2)}\right), \quad (7)$$

where $\beta = 2k\sqrt{1-k^2}\cos\theta_h$. The maximum ΔSNR is reached for $k = 1/\sqrt{2}$, $\cos\theta_h = \pm 1$, and $\cos\theta_t = \mp 1$ as

$$\Delta\text{SNR}_{\max} = -10\log_{10}\left(\frac{(1-|\alpha_t|)^2 + 1}{2(1-|\alpha_t|)^2}\right). \quad (8)$$

This is shown in Fig. 2, indicating < -13.6 dB crosstalk requirement to achieve the SNR loss lower than 0.2 dB.

The loss of SNR increases bit error rate (BER) of the detected signal. Theoretically, assuming that the error power spectral density is represented by additive white Gaussian noise (AWGN) and uniformly distributed among all constellation points, for example for 64-QAM and 256-QAM signals, SNR should be respectively 15 dB and 19 dB to achieve an average BER of 10^{-3} [12]. In practice, AM-AM and AM-PM distortions of the PA lead to larger errors at larger constellation points. Some theoretical and experimental investigations of the TX crosstalk effects on the MIMO system performance suggest an isolation requirement of roughly 20 dB for negligible performance degradation [5], [9], [13]. However, more accurate modeling and analysis are yet required for high-order and wideband modulation schemes used in 5G networks.

B. Circuit Techniques for Multi-Channel PA

It is desirable to integrate two or more PAs on a single chip to reduce the system cost and size. There are two major mechanisms of crosstalk in a dual-channel PA chip shown in Fig. 3. 1) coupling between metal traces in the matching networks of the two PAs, and 2) coupling through the substrate which can be modeled by a distributed resistive-capacitive network. It should also be mentioned that, in practice, there

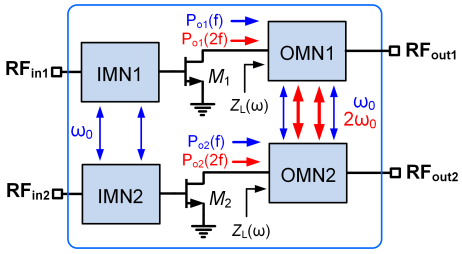

Fig. 3. Crosstalk in a dual-channel PA chip.

is substantial coupling between TX channels through the antenna networks. Although such antenna couplings cannot be mitigated using the on-chip circuit techniques, it should be considered in the MIMO TX crosstalk discussed.

We use two techniques to mitigate the substrate coupling. 1) Since the substrate coupling increases with frequency, crosstalk would be higher at harmonic frequencies (Fig. 3). Harmonic components coupled through the substrate not only degrade the linearity of the other channel, but also can be added to its harmonic contents with an unwanted phase and reduce the efficiency. A second-harmonic filter can be embedded into the PA output matching network to suppress its second-harmonic components before reaching the other channel. 2) The parasitic transformer coupling can be reduced by providing a large layout space between the two PA circuits. In this design, a minimum spacing of 300 μm is applied, which leads to an inter-channel transformer coupling coefficient of $k_m < 0.06$. Integrated GaN processes usually provide back-via through the substrate for grounding. This feature can be used to develop a shielding wall to reduce the substrate coupling (shown on chip micrograph in Fig. 4).

III. PA Circuit Design with Harmonic Filter

The PA is designed using a 250-nm GaN-on-SiC technology. The PA uses an $8 \times 125\,\mu$m gate-width transistor, with the drain supply voltage of 28 V, to be able to deliver 36 dBm output power. It is operated in the continuous class-B mode, where the extended design space for the optimum load impedance at the fundamental and second-harmonic frequencies helps to achieve high efficiency over a broad bandwidth [14]. In a narrow-band PA, the second harmonic could be readily suppressed at the output by incorporating a series or parallel resonant circuit into the matching network. In a broadband PA, however, this is a challenging task requiring trade-offs between bandwidth, insertion loss, and harmonic rejection in the output matching network. To this end, the output matching network is realized using a two-section minimum-inductance BPF with extra transmission zeros [8]. The circuit schematic of the two-channel PA is shown in Fig. 4, where a row of ground back-vias is used to mitigate crosstalk arising form the substrate and parasitic transformer couplings. EM simulations indicate that this technique reduces the crosstalk by ~2–7 dB across 4.0–7.0 GHz band.

The transistor gate bias exhibits significant effects on AM-AM and AM-PM distortions of the PA. In this design, a gate bias of -2.4 V is chosen to mitigate nonlinearity of the

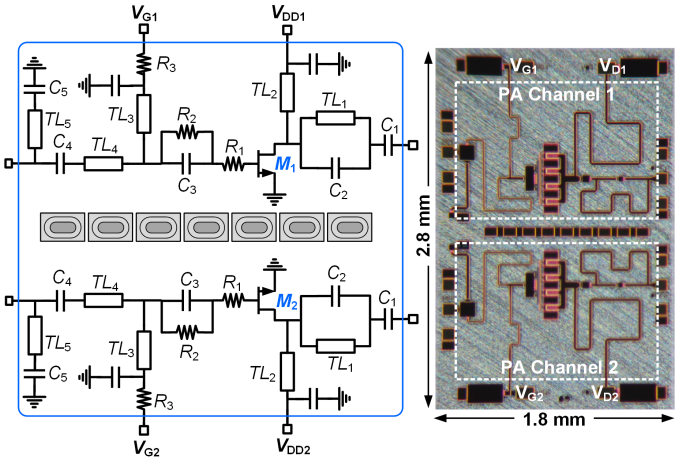

Fig. 4. Circuit schematic and chip micrograph of the two-channel PA. The size of transmission lines (width/length in μm) are TL_1: 25/1300, TL_2: 25/1950, TL_3: 17/800, TL_4: 15/1600, TL_5: 25/450, while C_{1-5}: 0.7, 0.4, 2.9, 3.0, 0.5 pF, R_{1-3}: 1, 9, 40 Ω, and $W_{M1,2}$: 8×125 μm.

transistor's transconductance and gate-source capacitance [7]. The PA delivers 35.4–36.4 dBm output power, 47–54% drain efficiency (DE), 44–50% PAE, and 11.4–12.4 dB power gain across 4.5–6.5 GHz. These results are achieved at 24 dBm input power. AM-AM and AM-PM are respectively 1.4 dB and $-3.2°$, up to 36.2 dBm output power at 5.0 GHz.

IV. Measurement Results

The PA is implemented using the 250-nm GaN-on-SiC process from WIN Semiconductors. The chip micrograph is shown in Fig. 4. The chip is mounted on the test PCB, and its bias and RF pads are wire-bonded to the PCB traces. The PA is characterized in single- and dual-channel operation modes using continuous-wave and modulated signals.

A. Single-Channel Measurements

The PA is biased at $V_{GS} = -2.4$ V and $V_{DS} = 28$ V, consuming 17 mA bias current. Measured output power, gain, DE, PAE, and second-harmonic rejection ratio (HRR2) versus frequency are shown in Fig. 5. The PA achieves 34.9–36.3 dBm output power, 11.3–12.3 dB gain, 48–52% DE, 44–49% PAE, and 31.0–34.2 dB HRR2 across the 4.5–6.5 GHz band. These results are measured at the input power of 24 dBm and 3–4 dB gain compression.

In Fig. 6, output constellation and spectrum of a single PA channel are shown for a 100-MHz 256-QAM signal with 7.2 dB PAPR at 5.0 GHz. The input power is adjusted to achieve EVM < -28 dB. The average output power, DE, and PAE are respectively 29.9 dBm, 33%, and 30%, while EVM is measured as -28.2 dB (3.9%). Also, adjacent channel leakage ratio (ACLR) of the output spectrum is $-38.2/-39.1$ dBc. By applying a DPD with an iterative learning control technique [15], EVM and ACLR can be respectively improved to -47.3 dB (0.43%) and $-47.5/-47.9$ dBc.

In Fig. 7, EVM, average DE, and ACLR are shown versus average output power for modulation bandwidths of 50 and

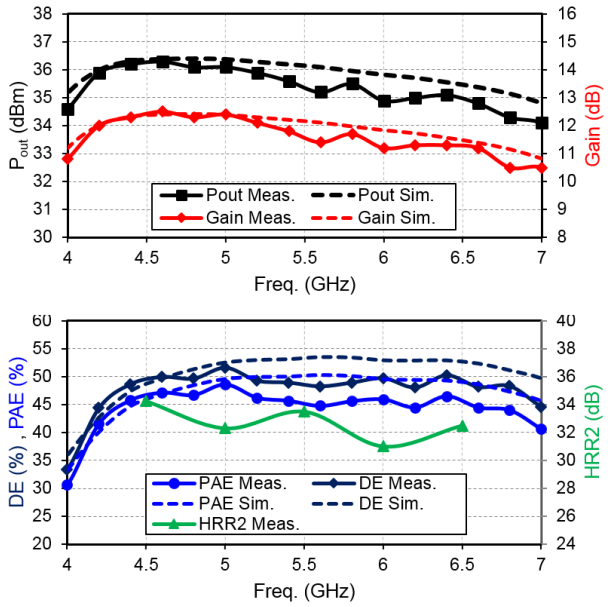

Fig. 5. Measured output power, gain, DE, PAE, and HRR2 versus frequency, at input power of 24 dBm.

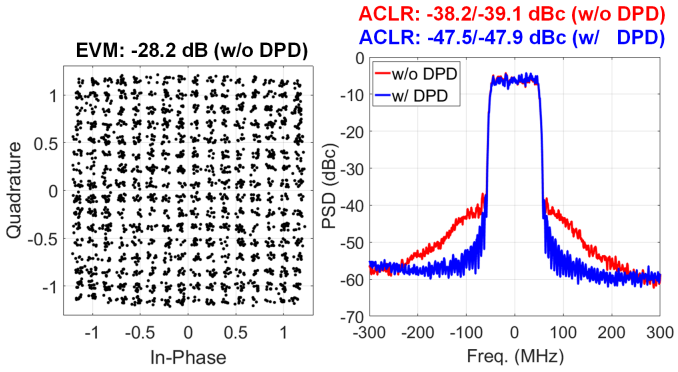

Fig. 6. Measured output constellation and spectrum for a 100-MHz 256-QAM 7.2-dB PAPR signal at 5.0 GHz. The output signal features 29.9 dBm average power and 5.6 dB PAPR.

100 MHz. Measured EVM is about 4 dB lower for the 50-MHz bandwidth in linear operation, but the difference becomes narrower as the output power increases. ACLR is slightly lower for the 50-MHz bandwidth, while average efficiency is almost the same for the two cases. EVM < -32 dB can only be achieved for 50-MHz 256-QAM signal with 29.8 dBm average output power and 29.5% average DE.

B. Dual-Channel Measurements

To measure the crosstalk between the two PA channels, the input power is applied to one of the channels (P_{in1}). Then, the direct output power in the same channel, $P_{out1} = G_{11}P_{in1}$, and the coupled output power in the second channel, $P_{out2} = G_{21}P_{in1}$, are recorded. This is a simplified approach to measure the crosstalk G_{21}/G_{11} using only *one* signal source. This measurement can capture nonlinearities in G_{11} and G_{21}, but excludes mutual nonlinearities, i.e., dependency of G_{11} and G_{21} on P_{in2}, are usually second-order effects. Such

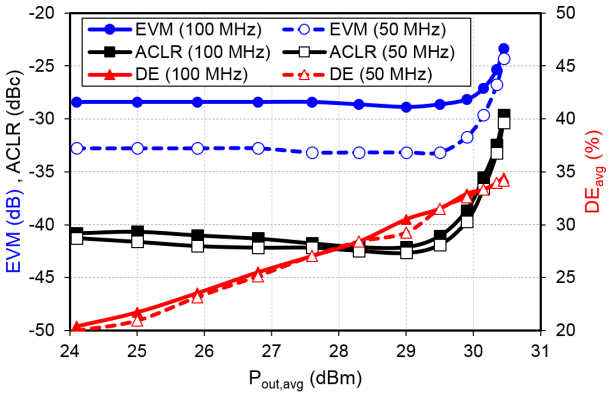

Fig. 7. Measured EVM, average DE, and ACLR versus average output power for a 50/100-MHz 256-QAM 7.2-dB PAPR signal at 5.0 GHz (w/o DPD).

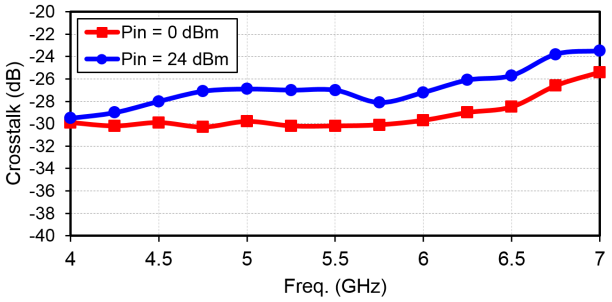

Fig. 8. Measured crosstalk between the two PA channels versus frequency at low/high input power levels.

mutual nonlinearities can be measured using a setup with two independent sources.

In Fig. 8, the measured crosstalk is shown versus output power. The crosstalk reads within -30.3 dB to -28.5 dB in low-power operation (0 dBm input) and -28.1 dB to -25.7 dB in high-power operation (24 dBm input). It is noted that < -25 dB crosstalk can be achieved which meets the requirements theoretically derived in Section II and the -20 dB limit suggested in the literature.

Test setup shown in Fig. 9 is used to measure the effect of crosstalk on the quality of modulated signals. The relative input power level to the two PA channels is varied using a 1-dB step attenuator[1]. The results are shown in Fig. 10 for a 50-MHz 256-QAM signal at 5.0 GHz. The EVM degrades as the input power to the other channel increases. The linear output power $P_{\mathrm{out,lin}}$, defined as the maximum average output power level for EVM < -28 dB, is 30.2 dBm for a single-channel PA. However, it reduces to 29.7 dBm when both channels operate at the same power, i.e., $\Delta P_{\mathrm{in}} = 0$ dB, and further degrades to 29.6/28.6 dBm for $\Delta P_{\mathrm{in}} = 3/6$ dB. Therefore, the PA should be operated in a bit stronger back-off in order to achieve the required linearity in the presence of crosstalk.

In Table I, the performance of the proposed dual-channel PA is summarized and compared with published broadband inte-

[1]A limitation of this test setup is correlation of the two modulated signals applied to the two PA channels. Two signal generators would be required to create the independently modulated signals, which was not available in this work. Furthermore, a phase shift should also be applied between the two inputs to represent the MIMO operation more accurately.

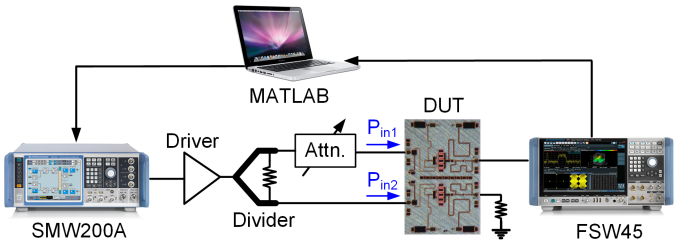

Fig. 9. Test setup to measure effect of crosstalk on EVM for modulated signals.

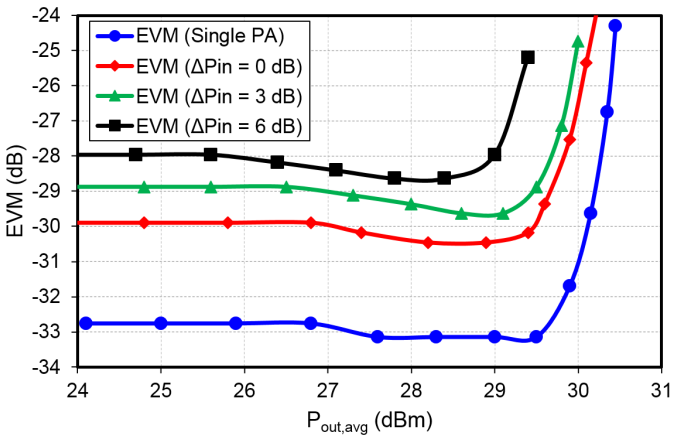

Fig. 10. Measured EVM versus average output power of a PA channel for different relative input power levels of the two channels. A 50-MHz 256-QAM 7.2-dB PAPR signal at 5.0 GHz (w/o DPD) is used in the measurements.

grated GaN PAs. To the best of authors' knowledge, there have been no reports of multi-channel PAs in this technology. The designed PA achieves high efficiency over a broad bandwidth, while having a compact chip area (2.5 mm^2 per channel) as an advantage of the proposed output matching network. EVM of -28.2 dB is achieved for a 256-QAM signal with a wide modulation bandwidth of 100 MHz to evaluate the PA linearity for 5G applications. A lower EVM of -32 dB can also be achieved for a 50-MHz modulation bandwidth and almost the same output power and efficiency.

V. Conclusion

We present a design approach for integrated dual-channel broadband power amplifiers (PAs). Effect of the transmitter crosstalk on performance of a 2×2 multi-input multi-output (MIMO) communication system is theoretically investigated for two popular coding schemes. The dual-channel PA adopts second-harmonic suppression and layout techniques (e.g., using a line of grounded back-vias) to mitigate crosstalk between the channels. A PA prototype implemented using a GaN-on-SiC process achieves >44 % power-added efficiency (PAE) and < -25 dB crosstalk across 4.5–6.5 GHz.

TABLE I
Summary of the Proposed Dual-Channel PA and Comparison with Broadband Fully Integrated Single-Channel GaN PAs

	This Work	[16]	[17]	[18]	[7]	[19]
BW (GHz)	4.5–6.5	4.9–5.9	6.8–7.2	4.9–5.9	4.6–6.0	6.4–8.3
P_o (dBm)	34.9–36.3	37–37.7	37.7–38.0	34.6–36.1	34.7–36.2	36–36.6
PAE (%)	44–49	48–55	58–64	49–61	42–52	36–47
Gain (dB)	10.6–12.4	28.5–31.7	12.2–13.5	8–12	12.2–13.4	10–12
Crosstalk (dB)	< -25.7	—	—	—	—	—
QAM order	256	256	256	256	256	256
BW_m (MHz)	100/50	80	60	80	100	7
PAPR (dB)	7.2	11.25	7	—	8.2	7.4
f_c (GHz)	5.0	5.7	7.0	5.2	5.0	7.0
EVM_{rms} (dB)	$-28.2/-32$	-32	—	-32	-28	—
$P_{o,avg}$ (dBm)	29.9/29.8	30.6	32	28	31.1	28.7
PAE_{avg} (%)	30/29.5	26	30	30	35	26
Area (mm^2)	2×2.5	4.7	9.0	2.4	2.2	7.8
Process (nm)	250	250	250	250	250	250

References

[1] E. G. Larsson, O. Edfors, F. Tufvesson and T. L. Marzetta, "Massive MIMO for next generation wireless systems," *IEEE Comm. Mag.*, vol. 52, no. 2, pp. 186–195, Feb. 2014.

[2] S. Shinjo *et al.*,"Integrating the front end: A highly integrated RF front end for high-SHF wide-band massive MIMO in 5G," *IEEE Microw. Mag.*, vol. 18, no. 5, pp. 31–40, July-Aug. 2017.

[3] H. Liao *et al.*, "A fully integrated 2 ×2 power amplifier for dual band MIMO 802.11n WLAN application using SiGe HBT technology," *IEEE J. Solid-State Circuits*, vol. 44, no. 5, pp. 1361–1371, May 2009.

[4] A. Afsahi, A. Behzad, V. Magoon and L. E. Larson, "Linearized dual-band power amplifiers with integrated baluns in 65 nm CMOS for a 2×2 802.11n MIMO WLAN SoC," *IEEE J. Solid-State Circuits*, vol. 45, no. 5, pp. 955–966, May 2010.

[5] Y. Palaskas *et al.*, "A 5-GHz 108-Mb/s 2 ×2 MIMO transceiver RFIC with fully integrated 20.5-dBm P_{1dB} power amplifiers in 90-nm CMOS," *IEEE J. Solid-State Circuits*, vol. 41, no. 12, pp. 2746–2756, Dec. 2006.

[6] P. M. Asbeck *et al.*, "Power amplifiers for mm-Wave 5G applications: Technology comparisons and CMOS-SOI demonstration circuits," *IEEE Trans. Microw. Theory Techn.*, vol. 67, no. 7, pp. 3099–3109, July 2019.

[7] G. Nikandish, R. B. Staszewski, and A. Zhu, "Design of highly linear broadband continuous mode GaN MMIC power amplifiers for 5G," *IEEE Access*, vol. 7, no. 1, pp. 57138–57150, Dec. 2019.

[8] G. Nikandish, R. B. Staszewski, and A. Zhu, "Broadband fully integrated GaN power amplifier with embedded minimum inductor bandpass filter and AM-PM compensation," *IEEE Solid-State Circuits Lett.*, vol. 2, no. 9, pp. 159–162, Sept. 2019.

[9] C. Yu *et al.*, "Full-angle digital predistortion of 5G millimeter-wave massive MIMO transmitters," *IEEE Trans. Microw. Theory Techn.*, vol. 67, no. 7, pp. 2847–2860, July 2019.

[10] S. M. Alamouti, "A simple transmit diversity technique for wireless communications," *IEEE J. Sel. Areas Commun.*, vol. 16, no. 8, pp. 1451–1458, Oct. 1998.

[11] M. Joham, W. Utschick and J. A. Nossek, "Linear transmit processing in MIMO communications systems," *IEEE Trans. Signal Process.*, vol. 53, no. 8, pp. 2700–2712, Aug. 2005.

[12] K. Cho and D. Yoon, "On the general BER expression of one- and two-dimensional amplitude modulations," *IEEE Trans. Commun.*, vol. 50, no. 7, pp. 1074–1080, Jul. 2002.

[13] Y. Jin and F. F. Dai, "Impact of transceiver RFIC impairments on MIMO system performance," *IEEE Trans. Ind. Electron.*, vol. 59, no. 1, pp. 538–549, Jan. 2012.

[14] S. C. Cripps, *RF Power Amplifiers for Wireless Communications*, 2nd ed. Boston, MA: Artech, 2006.

[15] J. Chani-Cahuana, P. N. Landin, C. Fager and T. Eriksson, "Iterative learning control for RF power amplifier linearization," *IEEE Trans. Microw. Theory Techn.*, vol. 64, no. 9, pp. 2778–2789, Sept. 2016.

[16] B. Liu *et al.*, "A fully integrated class-J GaN MMIC power amplifier for 5-GHz WLAN 802.11ax application," *IEEE Microw. Wireless Compon. Lett.*, vol. 28, no. 5, pp. 434–436, May 2018.

[17] R. Giofre, P. Colantonio and F. Giannini, "A design approach to maximize the efficiency vs. linearity trade-off in fixed and modulated load GaN power amplifiers," *IEEE Access*, vol. 6, pp. 9247–9255, Mar. 2018.

[18] B. Liu *et al.*, "A highly efficient fully integrated GaN power amplifier for 5-GHz WLAN 802.11ac application," *IEEE Microw. Wireless Compon. Lett.*, vol. 28, no. 5, pp. 437–439, May 2018.

[19] R. Quaglia *et al.*, "Linear GaN MMIC combined power amplifiers for 7-GHz microwave backhaul," *IEEE Trans. Microw. Theory Techn.*, vol. 62, no. 11, pp. 2700–2710, Nov. 2014.